Molecular Physics Reports vol. 39 (2004) 199-222

CHARGING PROCESSES OF Mn IONS IN $Li_2B_4O_7$:Mn SINGLE CRYSTAL AND GLASS SAMPLES UNDER the INFLUENCE OF γ-IRRADIATION AND ANNEALING

D. PODGÓRSKA[1], S.M. KACZMAREK[1], W. DROZDOWSKI[2], M. WABIA[1], M. KWAŚNY[3], S. WARCHOŁ[4], V.M. RIZAK[5]

[1] *Institute of Physics, University of Technology, Al. Piastów 48, 70-310 Szczecin, Poland*
[5] *Institute of Physics, N. Copernicus University, 5 Grudziądzka Str., 87-100 Toruń, Poland*
[3] *Institute of Optoelectronics, Military University of Technology, 2 Kaliski Str., 00-908 Warsaw, Poland*
[4] *Institute of Nuclear Chemistry and Technology, Dorodna 16, 03-195 Warsaw, Poland*
[5] *Uzhgorod National University, Uniwersytecka 21, 88-000 Uzhgorod Ukraine*

Abstract: Single crystals of $Li_2B_4O_7$ doped with Mn^{2+} (0.014 mol. %) and $Li_2B_4O_7$ glasses doped with Mn^{2+} (0.1 mol. %), have been investigated using EPR method at 9.4 GHz after two years from the growth. In both systems the *Mn* ion is found enter substantially for the Li^+ ion as Mn^{2+} and/or Mn^{1+}, and, probably for the B^{3+} ion or interstitial as Mn^{3+}. In consequence at least two types of the manganese ions arise in the EPR spectrum in the same range of magnetic field. The EPR spectrum of glass system exhibits three resonance signals, at g~2.00, g~2.68 and g~4,60 and is very similar to others reported for Mn^{2+} ions glass systems. The EPR spectrum of $Li_2B_4O_7$:Mn crystal reveals only g~2.00 and g~2.89 lines. Annealing in Ar atmosphere does not change the spectrum (g=1.97(8)) while irradiation with γ-quanta with a dose of $5*10^4$ Gy decreases to some extent the intensity of Mn^{2+} EPR signal (g=1.99±0.01) introducing new EPR line (g=2.14±0.01), giving evidence on formation of other (Mn^{1+}, Mn^{6+}, Mn^0) valence states of manganese, moreover, *F-type* and/or V_k color centers are formed. The optical investigations of "as-grown" and γ-irradiated samples were performed giving evidence on Mn^0 and Mn^{6+} formation in the crystal after γ-irradiation. Only 620 nm emission was observed in photoluminescence spectrum of the glass, while 430 nm and 610 nm emissions in radioluminescence spectrum of both systems. TL measurements of the crystal reveal the strong TL peak at about 95 K, assigned probably to F^+ center.

1. Introduction

$Li_2B_4O_7$ (LBO) crystal is a negative uniaxial crystal which belongs to the 4 mm point group and $I4_1cd$. (C^{12}_{4v}) space group of tetragonal symmetry (a=b=9.477 Å, c=10.286 Å). B-O mean distance is equal to 1.45 Å, *O-O* to 2.38 Å, and *Li-O* to 2.1 Å [1]. The structure of the crystal along c axis is presented in Fig. 1.

LBO melts congruently at 1190 K, so it may be grown by Czochralski [1] and Bridgman [2] methods. It is a piezoelectric material and has been studied as a substrate for surface acoustic wave (SAW) devices [3]. Microwave devices using surface acoustic waves are in common use for infra-red filters for color television and under signal processing elements. As for its optical properties, the second harmonic generation of YAG: Nd laser was examined by Kvon [4] and Furusawa [5] and it was reported that the nonlinear optical coefficient was small. Nonlinear optical properties of LBO in the UV range were demonstrated and commented on the fourth and fifth harmonic generation of a YAG: Nd laser in [6]. So far LBO has not been used as a primary laser host or gain medium.

This is because of the tight packing of the LBO single crystal lattice and the relatively large sizes of the dopant ions. This is a reason for which mainly transition metal ions are used as active dopants. Among other transition metal ions the divalent manganese is very often used in phosphors because of its broad emission, related to the crystal field transition $^4T_1$-$^6A_1$ in cubic symmetry [7].

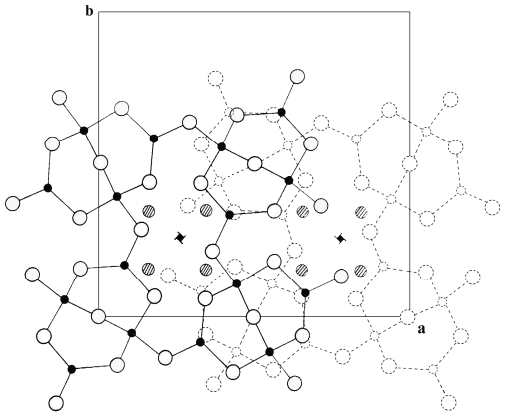

Fig. 1. Structure of LBO crystal along c-axis - B, - O, - Li

In weak crystalline fields, this broad emission band moves from green to red due to the increase at the cubic crystalline field *Dq*. Also the site symmetry strongly influences the emission spectra of Mn^{2+} ions [8]. Thus, depending on the host matrix, a variety of emission colors can be obtained [8-11]. However, because of the low oscillator strength of its *d-d* absorption transitions, crystals are usually co-activated with donor ions in order to excite the emitting Mn^{2+} ions by energy transfer in a more efficient way. LBO doped with Mn seems to be a promising thermoluminescent material because of its low phonon energy dependence [12], a radiation proof material for optical devices and a tissue-equivalent material for radiation dosimeter [13].

Owing to the small ionic radii of lithium and boron atoms, it is impossible to introduce dopants into $Li_2B_4O_7$ single crystals at high concentrations. A relatively high viscosity of molten lithium tetraborate, like of other borates, is a source of serious problems during single crystal growth of this material. On the other hand, this viscosity allows us to obtain the material in a form of glass containing much larger amounts of dopants than in case of single crystals [14, 15].

In both LBO:Mn single crystals and glasses the Mn^{2+} ions replace the monovalent *Li* cations and for the sake of local charge compensation, cation vacancies appear in the vicinity of Mn^{2+} ions, producing the so called impurity-vacancy (IV) dipoles.

In the present work we have investigated room temperature EPR spectra of LBO: Mn single crystals and glasses for "as-grown" materials, annealed in Ar-atmosphere, γ-irradiated with a dose of $5*10^4$ Gy and annealed in the air for 4h at 673 K, and also low temperature EPR spectra of the samples subjected to γ-irradiation, looking for possible Mn states and the exchange interaction between them.

2. Experimental

Single crystals of Mn doped LBO were obtained by Czochralski method in the Uzhgorod National University in Ukraina. Intentional concentration of Mn^{2+} in a single crystal was 0.014 mol %, while in glass 0.1 mol % [16].The standard materials were prepared by mixing Li_2CO_3 and B_2CO_3 powders at stoichiometric ratio of Li_2CO_3:B_2CO_3=1:2 for 24h. The dopant in the form of fine powder MnO_2 was added at 0.014 mol. % of the LBO charge. The as-grown crystals were transparent and had no visible bubbles and strips of defects. The synthesis of lithium tetraborate glasses was carried out from lithium carbonate Li_2CO_3, and boric oxide H_3BO_3 (Merck, extra pure) in platinum crucibles in air. After reaction of the starting materials at 1223 K, the obtained compound was overheated to 1423 K to remove traces of water and carbon dioxide, which were present in the melt. Because of B_2O_3 losses,

due to evaporation, 1 mol. % surplus of H_3BO_3 was added to the starting composition. After rapid cooling below 823 K, the melt formed glass which did not show any tendency to crystallize. Both type samples (LBO:Mn glass and LBO:Mn crystal) were investigated as "as-grown" ones, after two years from material growth.

Samples for EPR measurements had dimensions 2.2 x 2.2 x 2.1 mm^3 and 2.2 x 2.2 x 4 mm^3 for single crystal and glass, respectively. Electron paramagnetic resonance spectrometer was used working in the microwave X-band (~9.5 GHz). It was a Brucker E500 spectrometer of the CW-type (continuous wave) fully controlled by computer. It was equipped with an electromagnet capable of producing a stable magnetic field up to 1.4 T. An additional liquid helium flow cryostat produced by Oxford Instruments with a temperature controller enabling temperature variable studies of samples in the 3.5 – 350 K range was also applied.

A sample of LBO:Mn glass for optical measurements had dimensions 3 x 6 x 4 mm. It was measured for absorption, excitation and emission spectra before and after γ-ray irradiation with a dose of $5*10^4$ Gy. The irradiation's were carried out in the Institute of Nuclear Chemistry and Technology in Warsaw. Optical measurements were performed in the Institute of Optoelectronics, Military University of Technology, Warsaw using a LAMBDA-900 Perkin-Elmer spectrophotometer in UV-VIS-IR range. Values of $\Delta K(\lambda)$ due to the irradiation were calculated according to the formula:

$$\Delta K(\lambda) = \frac{1}{d} \cdot \ln \frac{T_1}{T_2}, \qquad (1)$$

where K is absorption, $\Delta K(\lambda)$ is additional absorption, λ is wavelength, d is sample thickness, and T_1 and T_2 are transmissions of the sample measured before and after the irradiation, respectively.

Photoluminescence measurements were carried out using a SS-900 Edinburgh Inc. spectrophotometer. Radioluminescence (RL) and low temperature thermoluminescence (TL) measurements were performed using a standard set-up consisting of an X-ray tube (DRON) operated at 42 kV and 10 mA, and a spectrograph, (SpectraPro-500i by Acton Research), equipped with a holographic grating (Hol-UV grating, 0th order, 2 mm slits), and a photomultiplier, PMT: Hamamatsu R928 (1000 V) for detection. The glow curves were recorded between 10 and 310 K at the hating rate of (0.148 ±0.001) K/s. Before the TL runs the samples were exposed to X-ray irradiation (DRON, 42 kV / 10 mA, 10 min).

3. Results

3.1. EPR investigations at room temperature

3.1.1. LBO:Mn single crystal

To check which changes take place in manganese valence states, the LBO:Mn crystal has been subsequently annealed at 923 K in argon for 5h, γ-irradiated with a dose of $5*10^4$ Gy and next annealed in the air for 4h at 673 K. Room temperature EPR spectra for "as-grown" crystal –"*a*", annealed in argon – "*b*" , γ-irradiated – "*c*" and annealed in the air – "*d*" are presented in Fig. 2. As one can see the EPR spectra for "as-grown" sample reveal typical spectrum related to six line hyperfine structure of Mn^{2+} impurity vacancy (IV) dipoles (g~2.0) (L_4 - line), superimposed on a rather broad background signal (L_1 – line), the envelope of all contributions at this absorption having g_{eff}~2.0 (Mn^{2+} ions at something different in symmetry sites, Mn^{1+} ions). The spectrum is characterised by a group of combined six pentads. The integral intensities of the Mn^{2+} pentad were found to be in good agreement with the theoretical intensity ratios 8:5:9:5:8. The same type of EPR spectrum is seen in Fig. 2d. Among Mn^{2+} lines one can distinguish close packed Mn^{2+} EPR lines coming from two at least different paramagnetic centres (see Fig. 2e). They may be Mn^{2+} pairs or clusters [17].

Fig. 2a).

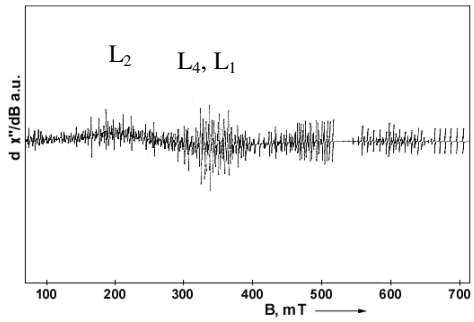

Fig. 2b).

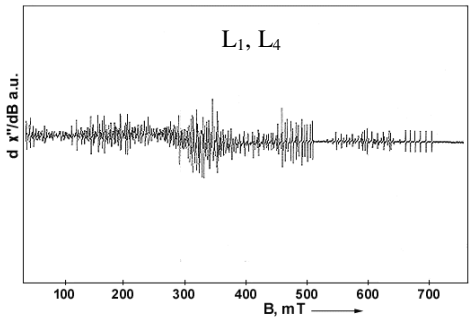

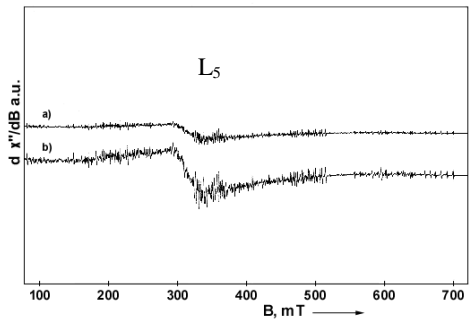

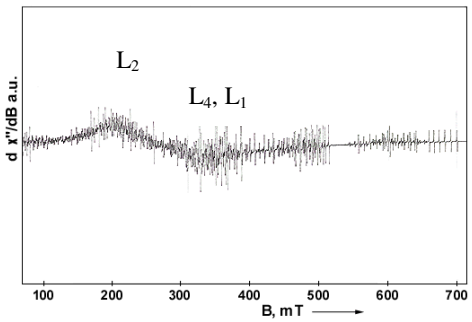

Fig. 2e).

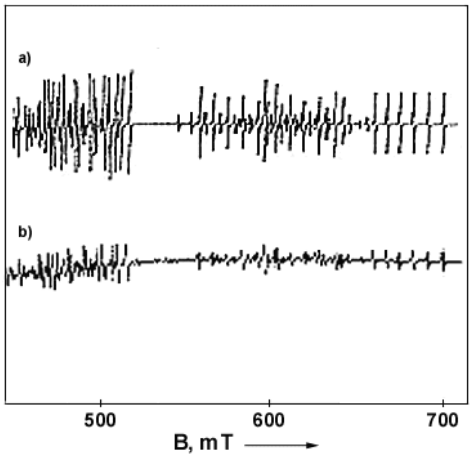

Fig. 2. RT EPR spectrum of LBO: Mn "as-grown" crystal at room temperature along *Z* axis (*Z*||*B*): 2a – a sample measured before annealing treatment, 2b – after annealing in Argon at 923 K for 5 h, 2c – after irradiation with γ-rays ($5*10^4$ Gy), 2d – after annealing in the air at 673 K for 4h, and 2e - a) "as-grown" crystal; b) γ-irradiated crystal; these are local magnifications of the curves plotted in Figs 2a and 2c, respectively; a) and b) curves of Fig 2c are plotted only for different values of the amplification of EPR spectrometer; ν=9.373 GHz

Moreover, the L_2 line one can also distinguish with g=2.89. Annealing in argon atmosphere (Fig. 2b) at 923 K does not change the structure of the spectrum (Mn^{2+}: g=1.97). For γ-irradiated sample (Fig. 2c), one of the set of lines disappear suggesting ionization effect to higher valence state of manganese ion (see the magnification of the EPR lines presented in Fig. 2e). Moreover, the intensity of the all Mn^{2+} lines decreases and new line arises (L_5, g=2.14), suggesting the presence of other type paramagnetic defects (e.g. Mn^0B). Annealing in the air (Fig. 2d) restores the EPR spectrum for as grown crystal. The line L_5 (Mn^{2+}: g =

2.14) deforms itself. To check which site positions are valid for Mn^{2+} in LBO:Mn^{2+} lattice we measured and calculated angle dependencies of Mn^{2+} lines. They are presented in Fig. 3.

3.1.2. LBO:Mn glass

LBO:Mn glass was investigated subsequently for "as-grown" sample, γ-irradiated ($5*10^4$ Gy) and annealed in the air.

Fig.3a) Fig.3b) Fig.3c)

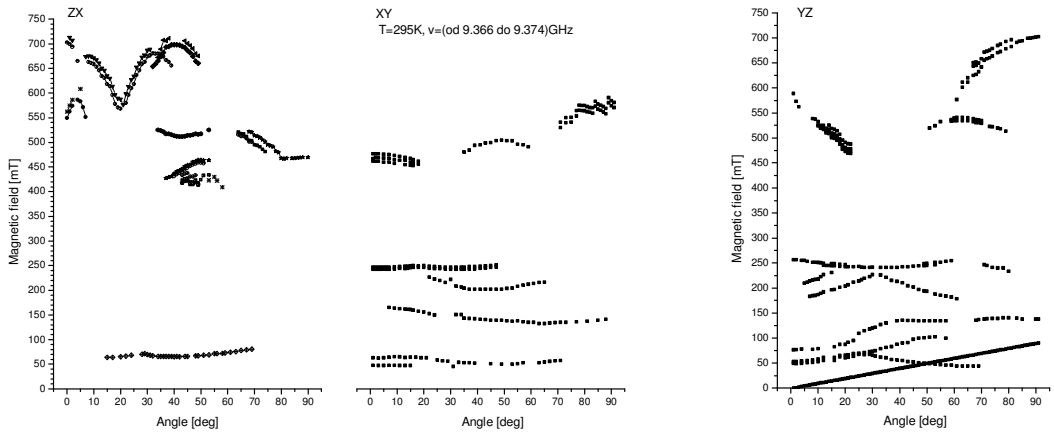

Fig. 3. RT angle dependencies for a) – *ZX* - plane, b – *XY* – plane and c – *YZ* – plane of LBO:Mn single crystal

Fig 4a). Fig. 4b).

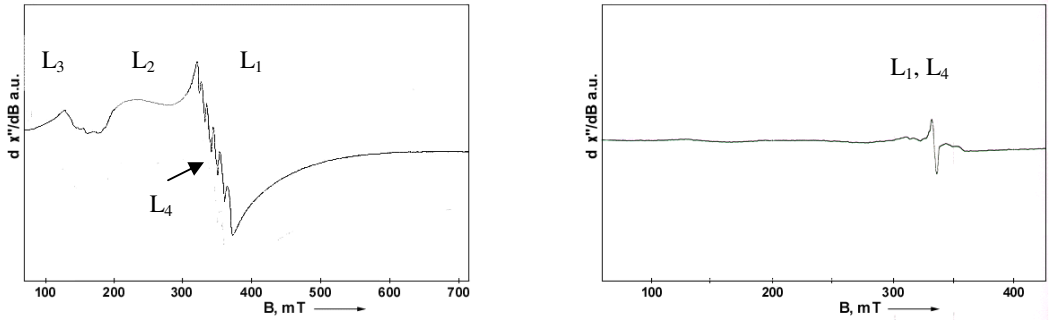

Fig 4c).

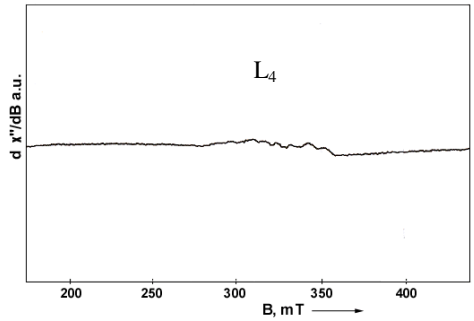

Fig. 4. RT EPR spectrum of LBO:Mn glass: a – "as-grown" sample, b – irradiated with gamma ($5*10^4$ Gy), and, annealed in the air for 4h at 673 K; ν = 9.389 GHz

The results of room temperature EPR measurements are presented in Fig. 4. As compared to the "as-grown" crystal, the "as-grown" glass shows EPR spectrum characteristic of Mn^{2+} ions with accompanying of other paramagnetic centers (broad exchange-narrowed line). In Fig. 4a one can distinguish L_1 (g~2.00), L_2 (g~2.68), L_3 (g~4.60) and L_4 (g~2.02) lines. All the lines seem to be attributed to manganese ions.

The EPR spectrum for γ-irradiated glass (Fig. 4b) differs in intensities of Mn^{2+} (L_4) and L_1 lines. These lines strongly decrease in intensity after γ-irradiation. After annealing in the air (Fig. 4c) L_1, L_2 and L_3 lines disappear and only single Mn^{2+} sixfold line (L_4 type) is observed, reciprocally as in case of LBO:Mn crystal.

3.2. Temperature dependence of EPR spectrum for γ-irradiated samples
3.2.1. LBO:Mn single crystal

To check the behaviour of the above lines as a function of temperature we have performed proper investigations for γ-irradiated samples. The results for LBO:Mn single crystal are shown in Fig. 5.

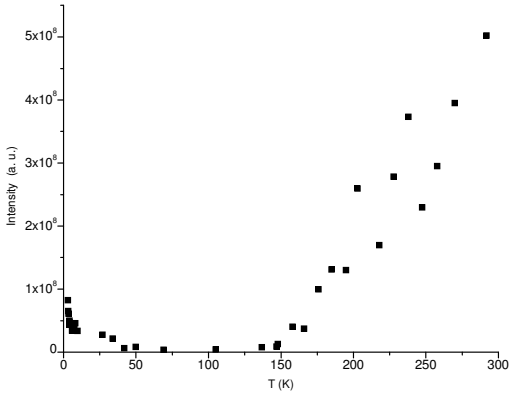

Fig. 5a. Temperature dependence of the integral intensity of L_5 EPR signal for LBO:Mn crystal

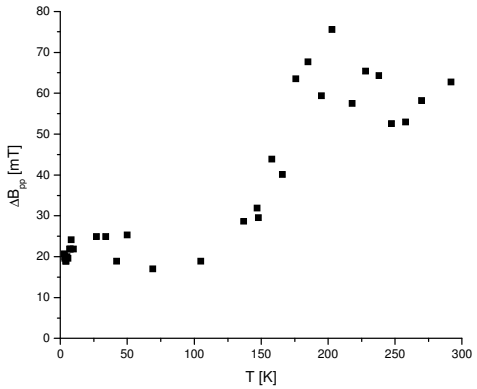

Fig. 5b. Temperature dependence of the L_5 peak-to-peak linewidth, ΔB, for LBO:Mn crystal

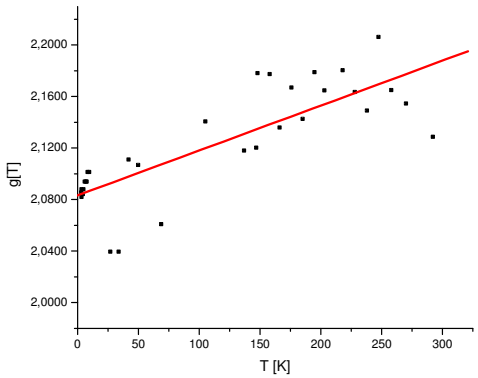

Fig. 5c. Temperature dependence of the g-factor for LBO:Mn crystal (line L_5)

As one can see from the Fig. 5a the integral intensity of EPR L_5 line decreases with the temperature for temperatures below 150 K while increases with temperature over 150 K. So,

both Curie and Curie-Weiss laws are not satisfied. The observed increase above 150 K may be attributed to the interchange interactions between paramagnetic centers, eg. Mn^0-Mn^{1+}-Mn^{2+}. Very similar behavior is observed for the temperature dependence of L_5 EPR linewidth (Fig. 5b), where the effect of the interchange interaction above 150 K is clearly seen.

3.2.2. LBO:Mn glass

The results for LBO:Mn glass are presented in Fig. 6. As one can see from Fig. 6a the all L_1, L_2 and L_3 lines reveal the same type of behaviour versus temperature. As compared to single crystal the peak-to-peak linewidth of L_1 EPR line is found to be independent of temperature for the glass (Fig. 6b), whereas the intensity of the line decreases with the increase in temperature (Fig. 6a) in all investigated range. The same behaviour we observe for g-factor (Fig. 6d). Corresponding characteristics for L_4 and L_3 lines show their increase with temperature.

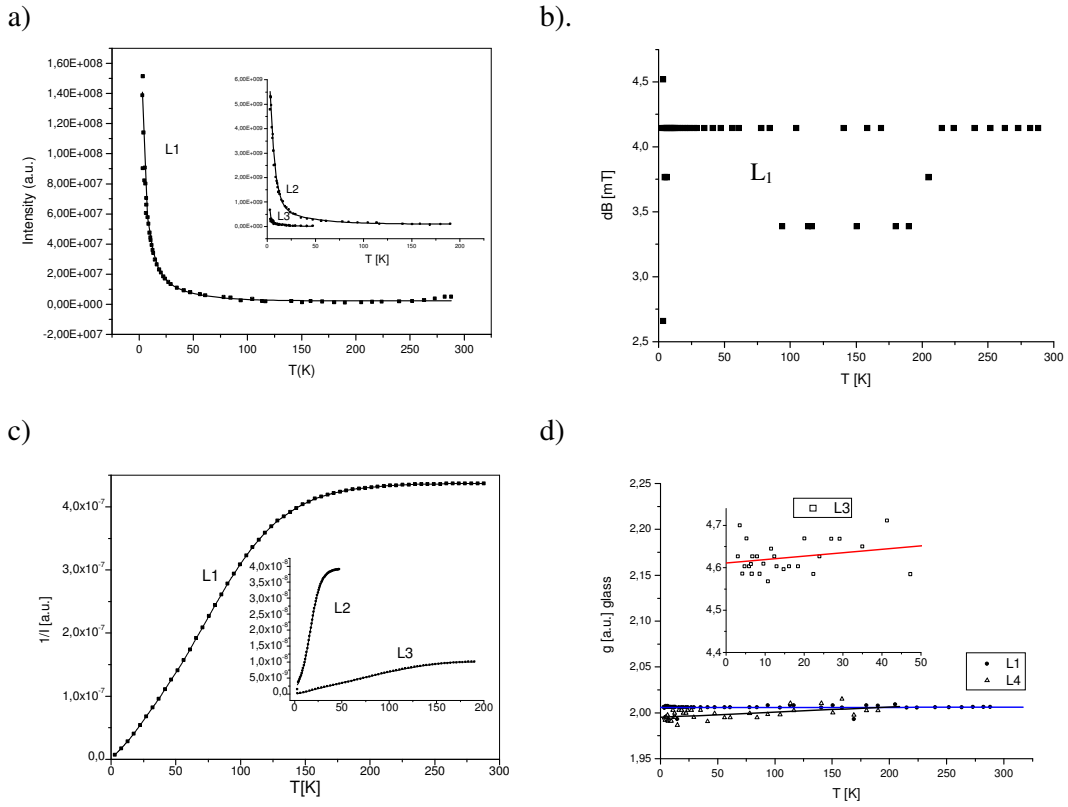

Fig. 6. a) EPR intensity I of L_1, L_2 and L_3 lines, b) - peak-to-peak linewidth ΔB of L_1 line, c) - $1/I$, d) - g factor versus temperature for LBO:Mn glass

3.3. Optical investigations
3.3.1. LBO:Mn^{2+} glass

Mn^{2+} ion gives rise to transition between crystal field energy levels within its $3d^5$ electronic configurations. Mn^{2+} has the free ion ground state, ^6S, the only spin sextet state, and it is not split by an octahedral crystal field. In an octahedral environment, in a weak crystal field ^6S transforms into $^6A_1(S)$ as the ground state, whereas ^4G splits into $^4T_1(G)$, $^4T_2(G)$, $^4E(G)$, $^4A_1(G)$ (see Fig. 7a). The absorption transitions are spin and parity forbidden in an octahedral environment. As a result, the absorption bands, especially for low doped crystals,

are very weak and the optical transitions of moderately Mn^{2+} doped crystals must be generally investigated by photoluminescence (excitation and emission technique).

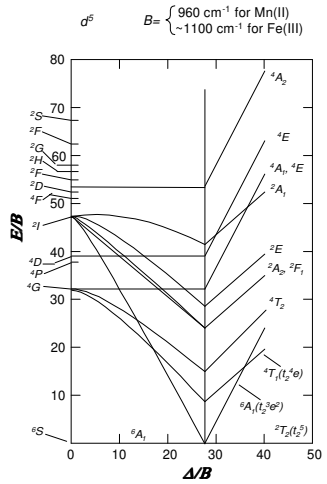

Fig. 7a). Tanabe-Sugano diagram of d^5 electronic configuration

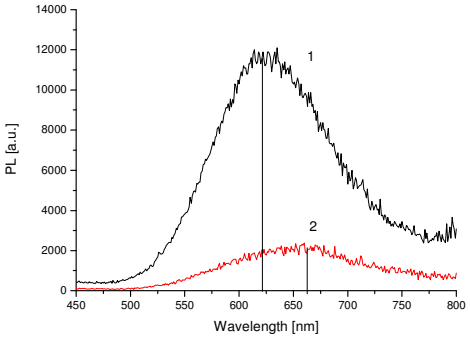

Fig. 7b). PL spectra of "as-grown" (1) , and γ-irradiated LBO:Mn glass sample; λ_{ex}=412 nm

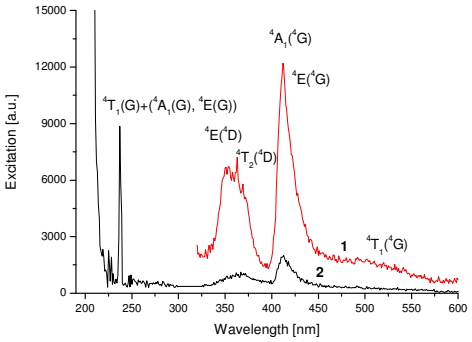

Fig. 7c). Excitation spectra of "as-grown" (1) and γ-irradiated LBO:Mn glass (2)

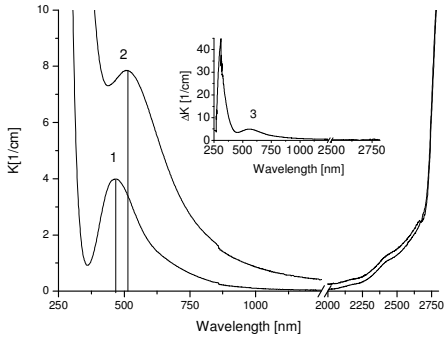

Fig. 7d). Absorption of "as-grown" (1), γ-irradiated (2) and additional absorption (3) of LBO:Mn glass

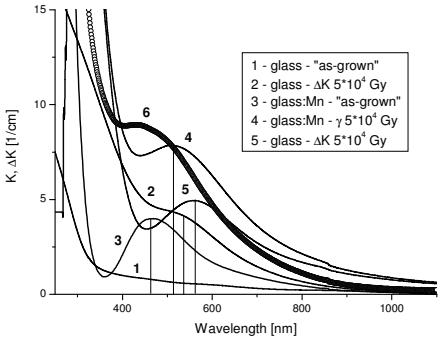

Fig. 7e). Absorption of "as-grown" pure glass (1), additional absorption of pure glass (2), absorption of "as-grown" LBO:Mn^{2+} glass (3), absorption of γ-irradiated LBO:Mn^{2+} glass (4), additional absorption of LBO:Mn^{2+} glass (5), and the sum of the absorption of LBO:Mn^{2+} glass and additional absorption of pure glass (6)

Fig. 7a presents Tanabe-Sugano diagram for d^5 configuration characteristic of Mn^{2+} ion (in case of LBO:Mn glass, Δ/B~12 and Dq/B~1,2). Fig. 7b shows the Mn^{2+} ion emission spectra observed for the "as-grown" (curve 1) and γ-irradiated with a dose of 10^5 Gy, LBO:Mn glass (curve 2). In both type glasses one broad emission band is observed; a red emission band around 620 nm for "as-grown" sample and a broader, red shifted emission band peaked around 660 nm for γ-irradiated one. So irradiation shifts red emission band of LBO:Mn glass by about 40 nm towards higher wavelengths. Moreover, the intensity of the emission is much lower for irradiated sample.

In order to gain additional information on the Mn^{2+} centres responsible for the observed emission bands, their corresponding excitation bands were recorded. In Fig. 7c) one can see these spectra in the wavelength range 200-600 nm (1 nm resolution).

In order to support the Mn recharging under γ-irradiation we performed analysis of the absorption spectra before and after the irradiation. As one can see from Fig. 7d), γ-irradiation leads to the increasing in the intensity of the 467 nm Mn^{2+} band and to the shifting of the band towards longer wavelengths (520 nm). Additional absorption band (curve 3) shows two main features. Strong induced absorption near the Fundamental Absorption Edge (FAE), centred at about 300 nm, and, the additional induced band centred at about 575 nm. To check which is reason such a shape of the absorption we have performed γ-irradiation of pure glass. In Fig. 7e) one can see the absorption of pure glass (curve 1), the induced absorption of the glass (2), the absorption of Mn^{2+} doped LBO glass (3), the absorption of γ-irradiated Mn^{2+} doped LBO glass (4), the induced absorption of γ-irradiated Mn^{2+} doped LBO glass (5), and, the sum of the absorption of LBO:Mn^{2+} glass and induced absorption of pure glass (6).

To check our hypothesis on possible explanation of L_1 and L_5 EPR lines by the presence of manganese clusters or precipitation's, we performed radioluminescence (RL) measurements of the LBO:Mn glass (the samples annealed in the air).

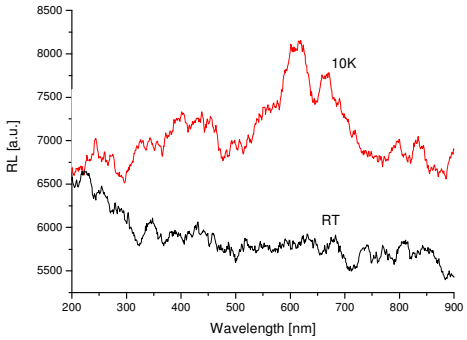

Fig. 8. RL spectra at RT and 10 K for LBO:Mn^{2+} glass

As one can see from the curves plotted in Fig. 8 both 430 and 610 nm RL emission bands are seen in the spectrum. Moreover, some other types of the emission arise above the 700 nm suggesting contribution of the higher valence states of manganese to the emission spectrum. Although the RT RL spectrum does not show any clear emissions, the low temperature spectrum evidently confirm our hypothesis. X-ray excited thermoluminescence (TL) glow curves have not shown any TL emission in case of the glasses. The obtained results confirm our conclusions resulting from PL spectra measurements in the glass after gamma irradiation. So in our LBO:Mn glass different states of manganese ions may be simultaneously present.

3.3.2. LBO:Mn crystals

The absorption spectrum of "as-grown" $Li_2B_4O_7$:Mn single crystal (see inset of Fig. 9) does not reveal the presence of clear Mn^{2+} absorption band, but one can observe strong unresolved band due to Mn^{2+} absorption and different growth defects in the UV-VIS part of the spectrum. The irradiation with γ-quanta changes the pattern giving much information about defect structure of the crystal. The induced absorption spectrum, shown in Fig. 9, reveals the presence of several bands peaking at: 225, 250, 370, 467, 480 and 610 nm.

Because in the EPR spectrum of gamma irradiated LBO:Mn single crystal the L_5 line arises, we recorded also RL spectrum for the crystal.

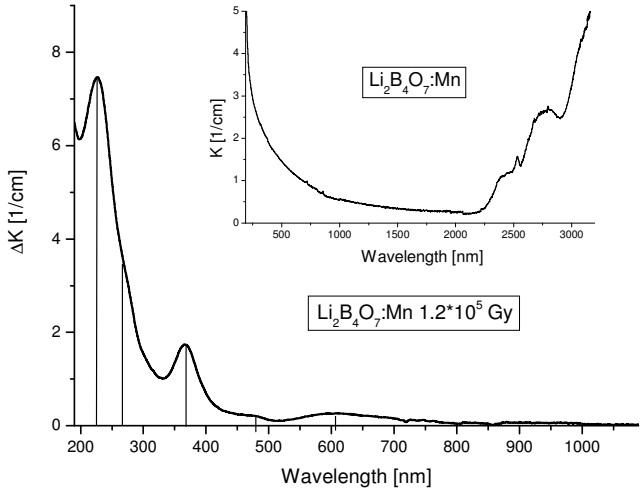

Fig. 9. Induced absorption bands in $Li_2B_4O_7$:Mn crystal after γ-ray irradiation with a dose of $1.2*10^5$ Gy; in the inset the absorption spectrum of the "as-grown" crystal is presented.

As one can see from Fig. 10, clear 430 (blue) and 610 nm (red) emission bands are observed, suggesting the presence some types of Mn^{2+} clusters in the crystal. Moreover, some other type of emissions is observed for wavelengths higher than 700 nm. We assign them to Mn^{4+} and Mn^{3+} ions emission [18].

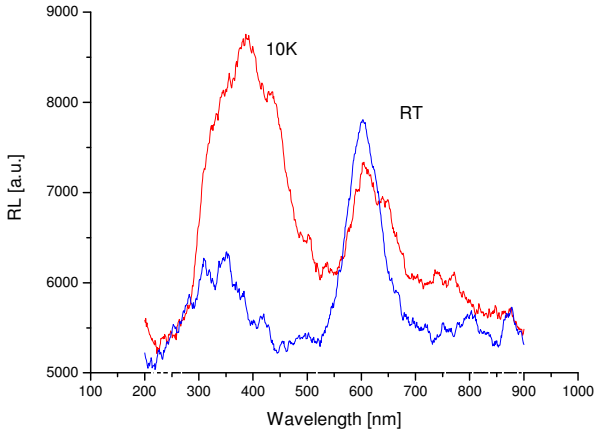

Fig. 10. RL spectrum of LBO:Mn single crystal at RT and 10 K.

The glow curve of the LBO:Mn single crystal is shown in Fig. 11. Low temperature TL measurements have revealed a rich TL spectrum with characteristic, extremely narrow peaks that give evidence on piezoelectric nature of LBO: Mn single crystal (see values of steady state RL). In the temperature range from 10 to 310 K we can distinguish, moreover, at least five TL peaks at about 95, 110, 130, 165 and 215 K that can be assigned to some types of traps (electron and hole types) present inside the band gap of our crystal. The TL glow curves were fitted, using the classic 1st order equation based on the Randall-Wilkins model [19] and the procedure described in detail by Drozdowski et al. [20]. The trap parameters, i.e. the depths E and frequency factors s, derived from the fitting procedure, are summarized in table 1. As one can see the results characterise four shallow traps of the depths E = 0.1-0.2 eV. We can assign them to F^+ or Mn^oB, V_k and Mn^{3+}, Mn^{6+} centres.

In Fig. 12 we have shown the dependence of the lifetimes of the four traps as a function of a temperature. The curves were calculated according to Arrhenius equation:

$$\tau^{-1} = \tau_0^{-1} \exp(-\Delta E/k_B T) \qquad (2)$$

where ΔE is the activation energy and k_B is the Boltzman constant.

4. Discussion

4.1. EPR results

The EPR spectrum of the investigated "as-grown" glass samples exhibit three resonance signals, at g~2.00 (L_4), g~2.68 (L_2) and g~4.60 (L_3) seen in Figs 2 and 4, suggesting rhombohedral distortion of manganese octahedral sites. For LBO:Mn crystal only L_1, L_2 and L_4 lines are observed, suggesting trygonal distortion of manganese octahedral sites. The EPR spectrum is very similar to others reported for Mn^{2+} ions systems [17, 21-24]. The resonance signal at g~2.00 (L_4 – line) show a six line hyperfine structure superimposed on a rather broad background signal (L_1 – line), the envelope of all contributions at this absorption having g_{eff}~2.0, also Mn^{2+} clustering [24]. The characteristic hyperfine structure (hfs) is due to the interaction of electron spin with the nuclear spin of the ^{55}Mn (I = 5/2) isotope and was resolved for the g~2.00 resonance line.

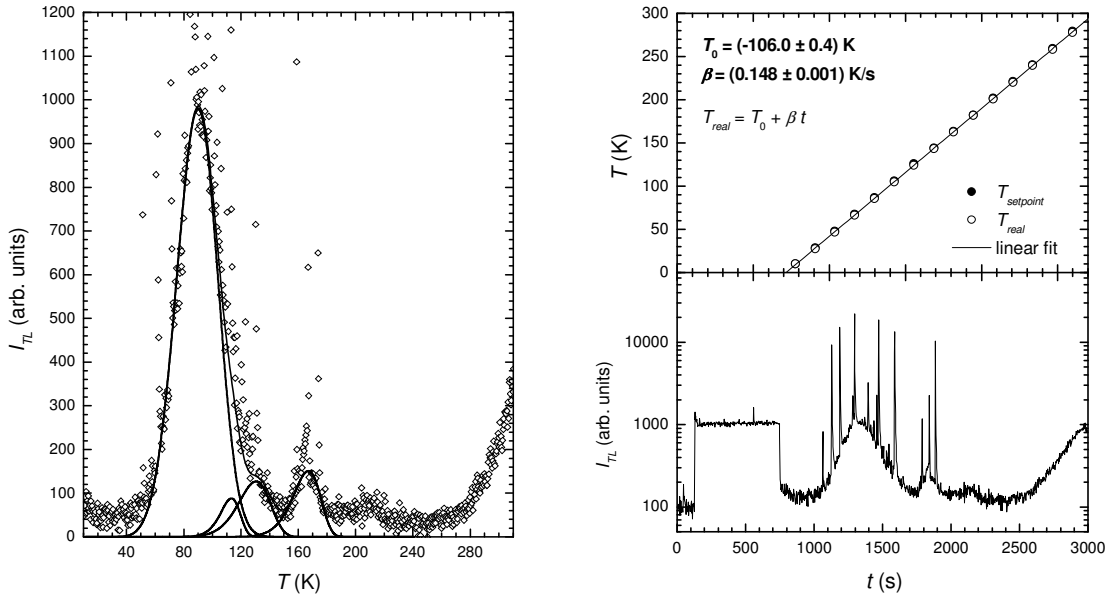

Fig. 11. a) X-ray TL curve and 1st order fit for LBO: Mn single crystals; b) temperature dependence and the steady-state RL

Table. 1 The initial concentrations, n_o, activation energies, E(eV), and, frequency factors, ln(s) of four traps occurring in the LBO: Mn single crystal, derived from the first-order glow curve fits.

type	n_o	E (eV)	ln (s)
1	2.120e+05	4.249e-02	8.821e-01
2	1.045e+04	1.540e-01	1.189e+01
3	2.379e+04	1.230e-01	6.567e+00
4	2.506e+04	2.398e-01	1.245e+01

In case of d^5 transition metal ions, it is known that axial distortion of octahedral symmetry gives rise to three Kramers doublets |±5/2>, |±3/2> and |±1/2> [25]. Application of the Zeeman field splits the spin degeneracy of the Kramers doublets. As the crystal field splitting is normally much greater than the Zeeman field, the resonance's observed are due to transitions within the Kramers doublets split by Zeeman field. The resonance's at g~2.68 and g~4.60 are attributed to the rhombic surroundings of the Mn^{2+} ions. The resonance at g~2.00 is due to Mn^{2+} ions in an environment close to octahedral symmetry and is known to arise from the transition between the energy levels of the lower doublet, while the resonances at g~2.68 and g~4.60 arise from the transition between the energy levels of the middle Kramers doublet.

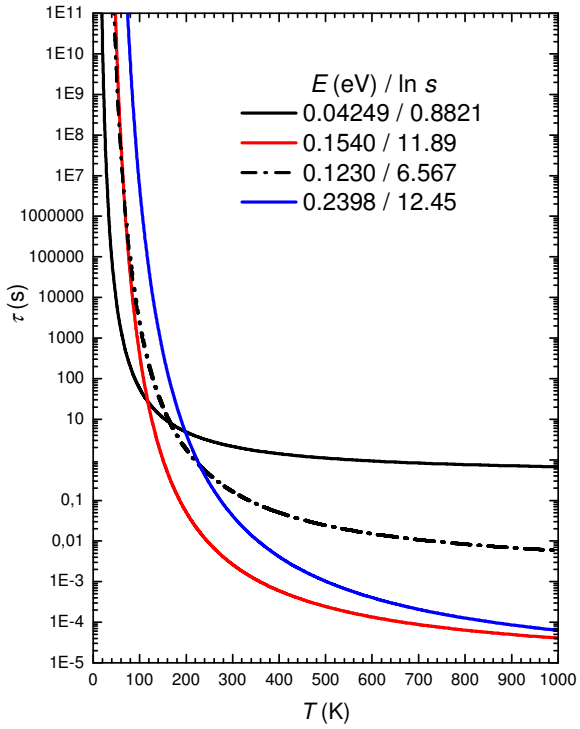

Fig. 12. The lifetimes of the four above mentioned traps as a function of a temperature

In ref. [24] it was found the g~4.3 resonance line registered for MnO-B_2O_3-PbO glasses is due to magnetically isolated Mn^{2+} ions in tetragonally distorted sites of octahedral symmetry. In case of low Mn concentrations (<1 mol%) of the glasses, the g~2.00 absorption being broaden structurless line may be attributed to all paramagnetic centres (manganese ions and

accidental impurities giving rise to g~2.00 resonance) while for higher concentration of Mn^{2+} (>5 mol%) it may be attributed to Mn^{2+} ions involved in clustered formations. For higher

manganese concentration the intensity of the line strongly depend on manganese concentration.

In ref. [17] the authors assigned the g~2,00 line registered for NaCl:Mn crystal to precipitates responsible for the green (505 nm) and red (610 nm) emissions observed in the as-grown crystal. One of these precipitates (related to the 610 nm emission) is the Suzuki phase while the structure and composition of the other precipitate were not found. In any case the EPR spectrum related to these precipitates indicates a strong magnetic coupling between Mn^{2+} ions in both precipitated phases.

We have analysed the EPR spectrum of Mn^{2+} doped LBO crystal and glass using spin-Hamiltonian for ions in octahedral symmetry [25]. For different electron transitions the EPR spectrum can be described by the following equations:

$$
\begin{gathered}
|\pm 5/2, m\rangle \Leftrightarrow |\pm 3/2, m\rangle \\
B = B_o \mp 4D \pm (4/3)(a-F) + 4E^2/B_o - A_{\|} m - A_{\perp}^2 (35/4 - m^2 \pm 4m)/2B_o, \\
|\pm 3/2, m\rangle \Leftrightarrow |\pm 1/2, m\rangle \\
B = B_o \mp 2D \mp (5/3)(a-F) + 5E^2/B_o - A_{\|} m - A_{\perp}^2 (35/4 - m^2 \pm 2m)/2B_o, \qquad (3) \\
|+1/2, m\rangle \Leftrightarrow |-1/2, m\rangle \\
B = B_o - 8E^2/B_o - A_{\|} m - A_{\perp}^2 (35/4 - m^2)/2B_o,
\end{gathered}
$$

Where g is the spectroscopic factor; $B_o = h\nu/\beta g$; ν – frequency, β – Bohr magneton, D, E, a, F – crystal field parameters; $A_{\|}$ and $A_{|\_}$ - components of hyperfine structure tensor $\boldsymbol{A}$. The following crystal field parameters were calculated for LBO:Mn crystal: D = 879±5 Gs, a-F = 0±1, $A_{\|}$ = -86±1 Gs, $A_{|\_}$ = 109±1 Gs, E = 57±3, E/D = 0,07, B_o=3300 Gs, and g = 2.00±0.01.

The EPR results obtained by us suggest that in the LBO:Mn single crystal, manganese enter substantially for Li^+ forming Mn^{2+} impurity vacancy dipoles (L_4 line) and also clusters (manganese pairs) (L_1 line). Some of the octahedral Li sites reveal trygonal distortion (L_2 – line). Under ionisation treatment colour centres are formed and some of the cluster particles change their valence state giving Mn^{2+}-Mn^{k+} pairs (k>=0) [21] (L_5 –line). The forming of the pairs and colour centres leads to the disappearing of impurity vacancy dipoles that are again seen in the EPR spectrum registered after annealing of the crystal in the air. The γ-irradiation leads to the "curing effect" with respect to the symmetry of site positions of Mn^{2+} ions (the decreasing of L_2 line). But this conclusion is valid only for the crystal previously annealed. Generally, irradiation introduces new radiation defects that damage the crystal. The annealing leads to restore of EPR spectra for "as-grown" sample suggesting the increase in the defect concentration.

Very similar, but sometimes quite different observation one can obtain for LBO:Mn glasses. Some of the octahedral Li sites are rhombohedrally distorted (L_2 and L_3 lines). Manganese pairs appear in "as-grown" glass but as compared to the "as-grown" single crystal they may be Mn^{2+}-Mn^{k+} (k>=2) pairs. The combined central L_1 line could be interpreted as a result of the presence of mixed aggregation states. We attribute the line to Mn^{k+} ions placed at B^{3+} sites or at interstitial, to the aggregates of Mn^{2+}, and, to F^+-centres. Irradiation of the glass

with gamma quanta leads to ionisation of the pairs and as a result we observe the decrease in Mn^{2+} concentration, confirmed by the decrease in the intensity of both Mn^{2+} and Mn^{k+} EPR lines (L_1 and L_4). The decreasing of L_2 and L_3 lines suggests "curing effect" with respect to the symmetry of site positions of Mn^{2+} ions. So one can state the γ-irradiation improves defect structure of the glass. The annealing in the air leads to the disappearing of L_1, L_2 and L_3 lines suggesting the further improving of the defect structure of the glass (F^+ centres vanish).

4.2. Optical properties of the LBO:Mn glass

Non-irradiated absorption spectrum of LBO:Mn glass reveals the following features: the FAE at about 270 nm (pure glass reveals the edge below 190 nm) and lattice absorption at about 2700 nm. In the range of 367 to 1200 nm strong asymmetric absorption band is observed centred at about 467 nm. The shape of the absorption band suggests the presence in the glass manganese ions with higher than 2 valence states.

The observed excitation spectrum consists of several crystal field transitions from the ground level $^6A_1(S)$ to other excited sublevels within the $3d^5$ electronic configuration of Mn^{2+} ion of octahedral symmetry. The excited levels of the different transitions, also their wavelength positions, are common for "as-grown" samples and irradiated samples, although their intensities are slightly different. They are larger for "as-grown" samples.

The highest excitation ultraviolet peak at about 237 nm could not be ascribed to any crystal field transition and it was associated to the double excitation $^6A_1(S)+^6A_1(S) \rightarrow {}^4T_1(G)+(^4A_1(G), {}^4E(G))$ arising from two close Mn^{2+} ions [26]. The 355 nm band is associated to the single $^4E(^4D)$ transition. Other excitation bands observed in "as-grown" and γ-irradiated samples are: $^4T_2(^4D)$ (363 nm), $^4A_1(^4G)$ (350 nm) and $^4E\ (^4G)$ (~ 412 nm), and, $^4T_1(^4G)$ (~ 467 nm). After γ-irradiation the intensity of the excitation bands decrease suggesting decrease in the content of Mn^{2+} ions. No one new transition arises in the UV-spectrum.

The irradiation with γ-quanta of LBO: Mn glass leads to arising of the strong additional absorption band (45 cm^{-1}) on the FAE, centred at about 300 nm. It is registered in the absorption spectrum of the γ-irradiated sample as the shift of the FAE by about 40 nm towards longer wavelengths. The band was previously reported in Ref. [27]. We think it is due to an ionisation of oxygen ions by γ-rays. Electron knocked out from the oxygen is trapped by B^{3+} ion giving B^{2+} one. It takes place for boron in BO_4 tetrahedron. The same mechanism was previously observed for $Ga^{3+}+ e \rightarrow Ga^{2+}$ transition in GaO_4 tetrahedron of $SrLaGa_3O_7$ crystal [22], and for $Si^{4+}+ e \rightarrow Si^{3+}$ transition in SiO_4 tetrahedron of Mg_2SiO_4 crystal [23].

The absorption spectra of the glass after gamma irradiation show, moreover, the increase in the absorption intensity of 467 nm band and also the shifting of the band towards longer wavelengths by about 50 nm (520 nm band). We think the increase is due to the γ-induced absorption of colour centres (F_2^+ – type centres) attributed to pure glass (520 nm). The shifting may be due to other radiation defects.

The F centre in oxides consists of two electrons trapped in an oxygen ion vacancy. This defect is the oxide analogue of the F^- centre in the alkali halides. Since the F-centre in its ground state is diamagnetic there is no EPR spectrum. The F^+ centres are the oxide isomorphs of the F-centre in the alkali halides – a single electron is trapped in an oxygen vacancy. This is un-paired electron so this centre reveal paramagnetic features. In some ways there remain serious questions related to the interpretation of some experimental results, because impurities compete with vacancies as traps for free carriers. Just which of the defects (F, F^+) predominates is determined by the relative concentration of anion vacancies and impurities

whose valence might be changed by trapping an electron. Roughly, both F and F^+ centres are produced when the total anion vacancy concentration is less then the total concentration of impurity traps. The F_2^+ centre is double oxygen vacancy with three electrons.

The γ-induced absorption band is centred at about 575 nm. It is a broad one, expanding over IR up to about 1250 nm, and, may be assigned, beside to F_2^+ centre, to ^5E-$^5T_2$ transition of Mn^{3+} ions (usually registered as centred at about 530 nm [18]), ^2E-$^4A_2$ transition of Mn^{4+} ions (usually registered as centred at about 480 nm [18]) and to the $^3T_1(t^2_2)$-$^3T_2(t_2e)$ transition in Mn^{5+} ions (usually peaked at about 650 nm [18]).

The $^4T_1 \rightarrow {}^6A_1(S)$ emission band, centred at about 620 nm, is shifted after γ-irradiation by about 40 nm towards longer wavelengths, due to probably energy transfer between $^4T_1$ band and the broad band of the F_2^+ colour centre. The expanding of the band over IR part of the emission spectrum may be assigned also to the emission from Mn^{4+} ions ($^4A_2$-^2E), and Mn^{3+} ions ($^5T_2$-^5E). Moreover, the intensity of the emission is lower as compared to non-irradiated glass due to lower concentration of Mn^{2+} ions present in the glass after γ-irradiation.

Irradiation can induce numerous changes in the physical properties of a glass. This may originate from atomic rearrangements which take place powered by the energy given up when electrons and holes recombine non-radiatively, or could be induced by any sort of radiation or particle bombardment capable of exciting electrons across the forbidden gap E_g into the conduction band [28]. Other type of defects must be essentially available in glasses to serve as electron and hole traps (e.g. X_2^- (e.g. O_2^-), H (interstitial X_2^-), V (hole trapped by cation vacancy) centres).

In our glasses they may be V_k centres arising as an effect of hole capture by double (manganese pairs) lithium vacancy arising as a consequence of Mn^{2+} ions substitution at Li sites or F-type colour centres arising by Compton electrons capture by oxygen vacancies. Ezz-Eldin et al. [27] have analysed colour centres in gamma-irradiated vanadium-containing alkali-borate glasses and found the gamma induced spectra reveal a very sharp band at about 400 nm and a second, less intense band, centred at about 520-580. Studies of alkali-borate glasses have been reported also by Beekenkamp [28]. Taking into account his explanation, the absorption spectra of alkali-borate glasses irradiated and measured at room temperature can be discussed as follows. When alkali is added to the glass, it goes into network-modifying positions, and each molecule of alkali oxide results in the formation of two nonbridging oxygens. The negative charge on the nonbridging oxygen is compensated by the presence of the alkali. The nonbridging oxygen ions shift the *FAE* of the unirradiated glass from the VUV to longer wavelength. The position and the height of the band was induced at about 480-830 nm, depending upon the type and concentration of alkali. This band is considerably less thermally stable than the hole centre bands, and its peak position has been found to be a linear function of the alkali ion field strength [28]. The atomic structure of the defect centres in these glasses generally consists of a hole trapped on oxygen bringing between 3- and 4-coordination boron.

The absorption spectra produced by the transition metal ion are affected by the electric field which the ion experiences due to the surrounding oxygen ions (the liquid field). This field varies according to the number and type of oxygen ions in the first coordination sphere, and this in turn depends on the glass composition. It is believed that, with the presence of impurities in the solid lattice, the optical and magnetic properties change. Multivalent impurities, such as transition metal ions, can easily trap electrons or holes when irradiated. New optical absorption bands may develop.

From the induced absorption analysis after the γ-irradiation of LBO: Mn glasses it results the induced absorption band at 520 nm may be most probably related to the F_2 (F_{2+}) centers.

This conclusion was confirmed by analogical investigations of pure LBO glasses. The broad induced band centred at 575 nm may be attributed to Mn^{4+}, Mn^{3+} and Mn^{5+} ions absorption as an effect of ionisation of Mn^{2+} ions.

The simultaneous presence of Mn^{2+} and Mn^{3+} ions in Bi_2O_3-GeO_2 glasses was previously reported in [24] basing on comparison of the composition dependence of molar Curie constant for theoretical and experimental curves. Their data show that the molar fractions of the Mn^{3+} ions is higher than that of Mn^{2+} ions, except the glass with low (1 mol.%) concentration of manganese ions. Similar results were obtained for lithium- and lead-borate glasses [29, 30]. It is interesting to note that manganese ions in Bi_2O_3-PbO glass matrix are only in Mn^{3+} valence state [31]. These data indicate that the glass matrix nature play an important role in distribution of valence states of manganese ions in oxide glasses. The magnetic data obtained by the authors may be explained if one accepts the participation of Mn^{2+}-Mn^{2+}, Mn^{3+}-Mn^{3+} and Mn^{2+}-Mn^{3+} magnetic exchange pairs. So the EPR L_1 line with g=2.00 registered for LBO:Mn "as-grown" and irradiated with γ-quanta glass, is a resolution of the all contributions from manganese ions with 2+, 3+, 4+ and 5+ valences and EPR signal of F^+ centres.

As results from our investigations, the annealing of the glass in the air leads to disappearing of the broad L_1 and other two L_2 and L_3 lines. We performed additional experiments for the LBO glasses registering the absorption spectrum before and after the annealing in the air at 450°C for 3h. The additional absorption band shows the bleaching of the spectrum in the range from 190 to 1100 nm. The obtained results explain the shape of the EPR spectrum registered after the annealing that contains only Mn^{2+} IV dipoles (L_4 line) (Fig. 4c) in terms of F-centres conversion. This conclusion stay in agreement with other given in Ref. [7]: a heat treatment above 670 K converts F^+ centres to F-centres (F_2^+ to F_2).

4.3. Optical properties of the LBO:Mn single crystal

The LBO crystal structure consists of two three-dimensional interlocking networks of the (B_4O_9) characteristic groups. The Li atoms are positioned in the channels along c-axis. Mn^{2+} ions substitutes for Li ions, so one can expect strong influence of Mn^{2+} doping on point defect creation in the crystal. On the other hand the incorporation of higher concentration of dopants is impossible due to large discrepancy between ion radius of Li and manganese.

The absorption spectrum of Mn doped LBO crystal reveals the FAE below 190 nm and the lattice absorption at about 3000 nm. In the absorption spectrum of LBO:Mn (0.014%) crystal there is not observed any Mn^{2+} absorption band. The LBO:Mn "as-grown" crystal does not show emission coming from Mn^{2+} ions due to low manganese concentration (0.014%) but RL spectra reveal wide blue and red emission bands suggesting the presence in the crystal some types of different defects, similarly as in case of LBO:Mn glass.

The γ-irradiation of $Li_2B_4O_7$:Mn single crystal show four additional absorption bands in the induced absorption spectrum. The 467 nm band we assigned to Mn^{2+} absorption, but there is observed a shoulder at 480 nm also, which together with other type of the shoulder centred at 250-290 nm (the superposition of the $^4A_2$-$^4A_1$ transition of Mn^{4+} ions [18]), may be attributed to Mn^{4+} absorption, 610 nm is probably attributed to F_{2+} colour centre [7], or, to $^3A_2$-$^3T_1$ (T_d) electric dipole allowed transition of Mn^{5+} [32], and, the broad band, peaked at 650 nm, to the $^3T_1(t^2_2)$-$^3T_2(t_2e)$ transition in Mn^{5+} ions [18].

The 225 and 370 nm bands are assigned probably to other valence states of the manganese. We can assign the former to Mn^oB centre (Mn^o substituting for Li^+ in off-centre position; Mn^o is formed as a result of the Compton electron capture by Mn^{1+} ion) [33], and, the latter to $Mn^{6+}(d^1)$ [34]. There is observed also a week broad absorption band with a

maximum at about 800 nm (usually attributed to Mn^{6+} (T_d) ^2E-$^2T_2$ ligand-field transition [35]). Ideally, a d^o configuration will contribute only a charge transfer band, a $d^1(Mn^{6+})$ configuration a single strong band, and a $d^2(Mn^{5+})$ configuration several possible bands [27].

It means the ions being recharged by γ-rays were substituted also at tetrahedral boron sites or interstitial. The 370 nm centre may also be assigned to F^+ colour centre [7]. It is possible, nevertheless, that the 225 and 370 nm centres are perturbed V_k centres [7] arising due to the lithium vacancy pair presence. So, after γ-irradiation, in both $Li_2B_4O_7$:Mn crystal and glass, one can observe many radiation-induced centres and the simultaneous presence of different manganese ions with different symmetry, that may interact each other.

The above results allow as taking a conclusion: we found the simultaneous presence of different valence states of manganese ions at different site symmetries in the crystal. This conclusion confirms the EPR results on interchange interactions in the crystal above 150 K between manganese ions at different states. The pattern is confirmed also by EPR results for angular dependencies (Fig. 3), where beside octahedral positions one can distinguish other type of symmetry sites, i.e. trigonally distorted octahedral ones. Different manganese valence states arise in the LBO:Mn crystal as an effect of photochemical reactions:

$Mn^{1+} + e^- \rightarrow Mn^o$, or, ionisation process:
$Mn^{2+} + \gamma \rightarrow Mn^{3+}, Mn^{4+}, Mn^{5+}, Mn^{6+}$

We have performed additional measurements of the absorption spectrum of LBO pure crystal before and after the annealing in the air at 450 ^oC for 3h. The additional absorption spectrum shows the increase in the absorption in the range of UV-VIS. It may be an explanation of the shape of the EPR spectrum registered after annealing of the LBO:Mn crystal in the air (Fig. 2d). The annealing introduces structural defects to the crystal sample, reciprocally to the glass sample.

4.4. RL and TL of LBO:Mn glass and crystal
4.4.1. RL measurements

The kinetics of nonequilibrium processes in lithium borates single crystals excited with synchrotron radiation were examined by Ogorodnikov et al. [36]. In the LBO:Mn crystal the luminescence can be excited effectively by photons with energy in the vicinity of the long-wavelength FAE, by roentgen or corpuscular radiation, and also through the recombination processes with the participation of the lattice defects. Origin of the luminescence is attributed rather to the radiative annihilation of self-trapped excitons (STE). Synchrotron radiation excited luminescence spectrum shows complex broad band in the spectral region from 250-500 nm with a maximum intensity at about 312-417 nm, which may be fitted by two principal gaussians at about 284 and 380 nm, respectively. The spectral positions and breaths of these sub-bands demonstrate a good reproducibility, whereas the ratio of their intensities depends strongly on various factors, among them the crystallographic orientation of a sample, temperature, intensity and polarisation of an exciting synchrotron radiation.

In case of our LT RL results one can conclude: the behaviour of the complex UV RL peak, seen in Fig. 8 for LBO:Mn glass, and in Fig. 10 for the LBO:Mn crystal, is of the same nature. So, the conclusion valid for the synchrotron radiation excitation is valid also for our case of X-ray excitation by DRON. The conclusion is: one can envisage that emission of LBO: Mn crystal may possibly be connected with an oscillator *Li-O* near the lattice defect, however, this requires the further detailed investigation in this field.

The RL spectrum presented in Figs 8 and 10 may be assigned also to some type of possible defects in LBO: Mn crystal – Mn^{2+} clusters (when manganese enters the matrix as agglomerates in disordered localities). For NaCl: Mn single crystal it was also observed sixfold EPR spectrum related to Mn^{2+} IV dipoles (g=2.0) (in quenched crystal) and broad contribution due to manganese precipitates (in the as-grown sample). The presence of two types of Mn^{2+} aggregates was assigned to the existence of green (505 nm) and red (610 nm) luminescence bands in the PL spectrum [17]. One of the aggregates types (presumably that related to the 610 nm emission) is the Suzuki phase.

In case of our crystal one can support the same type of precipitate (Suzuki phase) responsible for 610 nm emission band seen in RL spectrum of both LBO:Mn glass and crystal and in the PL spectrum of LBO:Mn glass.

4.4.2. TL measurements of LBO:Mn crystal

Thermoluminescence, is an optical phenomenon where light is emitted by heating crystals previously exposed to ionising radiation. The intensity of light as a function of temperature consists of a series of successive peaks, called glow peaks, which form structured bands often extending for several hundreds of ^{o}C. TL depends on the material, on the type of impurity, on radiation induced defect centres, dose and type of ionising radiation. Because of the latter two connections, TL is widely utilised in radiation dosimetry [37, 38] and in dating [39]. In general this emission of light is due to the recombination of electrons and holes which have been trapped in energy levels between the valence and conduction bands. Upon heating, these charges are activated in the two previous bands from where they may decay by releasing part of their energy in the form of light, and so a glow curve is generated. Temperature at which glow peaks occur depend on several factors which include the energy levels of the impurities in the material and of the defect centres generated by the ionising radiation. Because of the complexity of the phenomena involved, it has always been difficult, if not impossible, to associate the glow peaks with known impurities and well defined centres.

Dosimetric properties of lithium tetraborate crystals were investigated in several papers. El-Faramway et al. have examined copper doped LBO crystal [40]. This relatively new TL material was found to have low fading, sensitivity and high dose response. *Mn*, *Cu* and *Mg* doped LBO crystals were investigated by K. Park et al. [41]. They stated the advantage of LBO crystals doped with *Mn* and *Mg* compared with sample doped with *Cu* is its simple glow curve with one main peak (473 and 523 K, respectively), and its temperature position depends to some extent on the exposure level. The material (*Mn*, *Mg* doped LBO) does not exhibit complicated trap dynamics and thus does not require complicated annealing procedures to obtain good reproducibility. For the *Mn*-doped sample, sensitivity was observed which is 100 times higher than that of the *Mg*-doped crystal.

We have not registered a paper devoted to low temperature (LT) TL measurements of LBO: Mn crystal. Fig. 11 shows the TL glow curves for LBO:Mn single crystal after 10 min of X-radiation. In the spectrum five glow peaks are observed, at: 95, 110, 130, 165 and 215 K, although the peak at 95 K is much more intense than the other three. The Randall-Wilkins analysis of the peaks has given the values of the activation energy of the traps responsible for the peaks of the order of 0.2 eV (shallow traps). To find the trap parameters we used the Randall-Wilkins formula:

$$I(T) = \sum_{i=1}^{4} n_{oi} s_i ep(-\frac{E_i}{k_B T}) \exp(-\frac{s_i}{\beta} \int_{T_o}^{T} \exp(-\frac{E_i}{k_B T}) dT), \quad (4)$$

where *I(T)* is the TL intensity at the temperature T, β is the heating rate; other notifications are described in the table 1. This expression was fitted to experimental points for LBO: Mn.

Very similar pattern for the TL glow curves was obtained by Lopez et al. [33] in case of NaCl: Mn single crystal. They observed 108, 171 and 222 TL peaks. The first of them they assigned to the following mechanism:

$$Mn^{3+} + e^{-} \rightarrow (Mn^{2+})^{*} \rightarrow Mn^{2+} + h\nu\,(585\ \text{nm}) \quad (5)$$

The electron may come from some unknown shallow trap.

The temperature of the second peak very closely agrees with that corresponding to the mobility of the V_k centers (self trapped holes). It has been clearly shown that this peak is associated to the annihilation of Mn^0B centers. A reasonable mechanism involves the tunneling of an electron from the Mn^{1+} (or Mn^0) ion to nearby V_k center, to form an excited self-trapped exciton $(V_k + e)^*$ next to impurity. The radiative decay of this exciton would yield one of the intrinsic emissions perturbed or made allowed by the impurity. Therefore the whole process can be outlined as follows:

$$\begin{array}{ccccc} & {\scriptstyle +V_k} & {\scriptstyle +V_k} & & \\ Mn^0 \rightarrow & Mn^{1+} & \rightarrow (Mn^{2+})^{*} & + & (V_k\ e)^{*} \\ & & \downarrow & & \downarrow \\ & & Mn^{2+} + h\nu\,(595\ \text{nm}) & & h\nu\,(410\ \text{nm}) \end{array} \quad (6)$$

The third peak at 222 K was attributed also to an annihilation of Mn^0B centers.

By comparing the results to these obtained by us one can conclude the 110, 165 and 215 K TL peaks registered for LBO: Mn crystal corresponds to 108, 171 and 222 K peaks registered for NaCl: Mn crystal. So their origin may be the same. The arising of both Mn^0B and Mn^{3+} centers in γ-irradiated samples was confirmed by optical investigations. Nevertheless there are observed in the TL spectrum of LBO: Mn crystal two new peaks at 130 K and more intense one at 95 K. The origin of the peaks is not clear and demand further investigations. Bearing in the mind possible defects present in the crystal after gamma irradiation, we can assign them to *F*-type color centers (F^+ and/or F_2^+).

So the results of TL measurements confirm our previous conclusions on the Mn^{1+} ions present in the "as-grown" crystal.

From Fig. 11 it results, moreover, the ratio of the intensities: TL/(steady-state + TL) = 0.6, so only about 40% of all the radiation-induced centres recombine thus after X-ray irradiation, while about 60% of the centres is firstly trapped.

From the above investigations it results there are present many types of point defects in the "as-grown" LBO:Mn single crystal. We can expect the presence some oxygen vacancies, nonbridging oxygens, un-controlled impurities and also *Li* vacancies, because substituting of Li^+ for Mn^{2+} demand the lithium vacancy for charge compensation, moreover, some types of Mn^{2+} clusters [17]. Some of them are seen as colour centres in the induced by γ-rays absorption spectrum (although dominating phenomenon is the recharging of manganese ions), and, some of them (shallow traps) were calculated using Randall-Wilkins procedure for TL

peaks. The strong TL peak registered at about 95 K may be assigned to F^+ and/or F_2^+ centres [7]. If we suppose the presence of e.g. F^+ centre than in the ESR spectrum of the centre a broad isotropic ESR line (similar to L_1 observed line) is expected to arise, the envelope of which is made up of many closely spaced hyperfine lines. The spectroscopic splitting factor, g, is isotropic for F-centres and very close to the free-electron value g=2.00.

The nature and the processes of the radiation defects formation in LBO crystals were not studied completely. Burak et al. [13] examined neutron-irradiated LBO crystals and have found F^+, O_2^- and O^- paramagnetic centres in newly grown and annealed in H_2 LBO crystal and also four types of other paramagnetic defects (*K1*, *K6*, (*K5*, *K8*) and *K9* – the *K*-band lays on the high-energy wing of the *F*-band and is strongly related to the band) [42], stable at room temperature (their g factor is being very close to 2.00) in neutron-irradiated samples.

5. Conclusions

The EPR spectrum of the investigated glass samples exhibit three resonance signals, at g~2.00 (L_4), g~2.68 (L_2) and g~4.60 (L_3) seen in Figs 2 and 4. It suggests rhombohedral distortion of octahedral *Li* sites. For LBO:Mn crystal only L_1, L_2 and L_4 lines are observed. It suggests trygonal distortion of *Li* sites. The EPR spectrum is very similar to others reported for Mn^{2+} ions systems [17-22]. The resonance signal at g~2.00 show a six line hyperfine structure superimposed on a rather broad background signal (L_1 – line), the envelope of all contributions at this absorption having g_{eff} ~ 2.0, e.g. F^+, V_k , F_{2+} colour centres, and also Mn^{k+} (k>1) clustering [24]. The characteristic hyperfine structure (hfs) is due to the interaction of electron spin with the nuclear spin I = 5/2 and was resolved for the g ~ 2.00 resonance line.

The annealing of the LBO:Mn crystal in argon atmosphere at 923 K does not change EPR spectrum of single crystal (the competition take place between the "curing" by reduction process and the damaging by the annealing one). The gamma irradiation "cures" the crystal from the point defects, giving additional L_5 EPR line attributed to Mn^0B centres. The annealing of the crystal in the air performed subsequently after previous γ-irradiation restores "as-grown" EPR spectrum (we observe the damaging of the crystal as an effect of the annealing, also clustering).

The gamma irradiation of the LBO:Mn glass "cures" the glass from point defects (lithium or oxygen vacancies) ionising Mn^{1+}, Mn^{2+}, and Mn^{3+} ions and converting *F*-centres. The annealing of the LBO:Mn glass in the air at 673 K completely changes EPR spectra giving evidence on the existing of only isolated Mn^{2+} ions (we observe the curing of the glass from point defects (conversion of F_2^+ centres) and clusters).

In the $Li_2B_4O_7$ single crystal Mn^{2+} is found enter substantially for the Li^+ ion. There are present also Mn^{1+} (at *Li* sites) ions and Mn^{3+} ions (at B^{3+} sites or at interstitial). In the LBO:Mn^{2+} crystal we observed Mn^{2+}-Mn^{k+} (k>=0) pairs together with IV dipoles (isolated Mn^{2+} ions). Gamma irradiated crystal shows the absorption bands suggesting the presence of Mn^0, Mn^{4+}, Mn^{5+}, and Mn^{6+} centres.

In the LBO: Mn glass, manganese ions substitute both octahedral Li^+ and tetrahedral B^{3+} sites and also interstitial as Mn^{2+} and Mn^{3+}. In the LBO:Mn^{2+} glasses we observed Mn^{2+}-Mn^{k+} (k>=2) pairs together with IV dipoles. Gamma irradiated glass shows the absorption spectra suggesting the presence of Mn^{4+} and Mn^{5+} centres.

In Mn^{2+} doped "as-grown" LBO single crystals and glasses there arises oxygen, and, Li^+ vacancies compensating Mn^{2+} substitution for Li^+.

Non-irradiated absorption spectrum of LBO:Mn glass reveals clear absorption bands characteristic of Mn^{2+} ions. Excitation spectrum shows the presence of the five main electronic transitions responsible for $^4T_1 \rightarrow {}^6A_1(S)$ emission observed in PL spectrum. They are: the highest excitation ultraviolet peak at about 237 nm associated to the double excitation $^6A_1(S)+{}^6A_1(S)\rightarrow{}^4T_1(G)+({}^4A_1(G),\ {}^4E(G))$ arising from two close Mn^{2+} ions, the 355 nm band associated to the single $^4E(^4D)$ transition, $^4T_2(^4D)$ (363 nm), $^4A_1(^4G)$ (350 nm) and $^4E\ (^4G)$ (~ 412 nm), and, $^4T_1(^4G)$ (~467 nm).

The irradiation with γ-quanta of the LBO:Mn glass leads to arising of strong additional absorption band (45 cm^{-1}) on the FAE (300 nm). We think it may be due to an ionisation of oxygen ions. Electrons knocked out from the oxygen are trapped by B^{3+} ions giving B^{2+} ones.

In the absorption spectrum of LBO:Mn (0.014%) crystal there is not observed Mn^{2+} absorption band. So, LBO:Mn "as-grown" crystal does not show emission coming from Mn^{2+} ions. It is due to low manganese concentration (0.014%). But *RL* spectra reveal wide blue and red emission bands suggesting the presence in the crystal some types of different defects among them Mn^{2+} clusters (Suzuki phase), similarly as in case of LBO:Mn glass.

The γ-irradiation of $Li_2B_4O_7$:Mn single crystal gives rise to conclusion: we found simultaneous presence of different valence states of manganese ions at different site symmetries (tetrahedral and octahedral) in the crystal. Ionisation leads also to V_k and/or F^+-type colour centres and/or Mn^{5+}, Mn^{6+} centres formation.

Low temperature TL measurements have revealed a rich TL spectrum with characteristic narrow peaks that give evidence on piezoelectric nature of LBO:Mn single crystal. In the temperature range from 10 to 310 K we distinguished, moreover, at least five TL peaks that are associated with some types of electron traps present inside band gap of our crystal. The energy depths and concentrations of the traps were calculated using Randall-Wilkins procedure. The higher TL peak registered at about 95 K may be attributed to F^+ colour centre. The origin of other peaks was assigned to Mn^{3+} and Mn^0 ions present in the irradiated crystals.

References

[1] D.S. Robertson and I.M. Young*, J. Mater. Sci*. 17 (1982) 1729
[2] S.J. Fan, W. Wang, J.J. Xiang and J.K. Xu, *J. Cryst. Growth* 99 (1990) 811
[3] R.W. Whatmore, N.M. Sharrocks, C.O. Hara, F.W. Ainger and I.W. Young*, Electron. Lett*. 17 (1981) 11
[4] T.Y. Kvon, J.J. Ju, J. W. Cha, J.N. Kim and S.I. Yun, *Material Letters*, 20 (1994) 211
[5] S. Furusawa, O. Chikagawa, S. Tange, T. Ishidate, H. Orihara, Y. Ishibashi and K. Miwa, *J. Phys. Soc. Jpn*, 60 (1991) 2691
[6] R. Komatsu, T. Suagawara, K. Sassa, N. Sarukura, Z. Liu, S. Izumida, Y. Segawa, S. Uda, T. Fukuda and K. Yamanouchi, *Appl. Phys. Lett*., 70 (1997) 3492
[7] B. Henderson, G.F. Imbush, *Optical Interaction of Inorganic Solids*, Clarendon Press, Oxford, 1989
[8] U. Lanver and G. Lehmann*, J. Lumin*. 17 (1978) 225
[9] J. Ramirez-Serrano, E. Madrigal, F. Ramos and G.U. Caldino, *J. Lumin*. 71 (1997) 169
[10] G.U. Caldino and O.J. Rubio, *Radiat. Eff. Defects Solids* 127 (1993) 83
[11] R. Clause and K. Petermann, *IEEE, J. Quantum Electron*., 24 (1988) 1114
[12] B. Chandra and R.C. Bhatt, *Instr. Methods*, 184 (1981) 557
[13] Ya. V. Burak, B.V. Padlyak, V.M. Shevel, *Nucl. Instrum. Methods* 191 (2002) 633
[14] Y. Anzai, K. Terashima and . Kimura, *J. Cryst. Growth*, 134 (1993) 235

[15] R. Komatsu, T. Sugihara and S. Uda, *Jpn. J. Appl. Phys*. 33 (1994) 5533; R.S. de Biasi, M.L.N. Grillo, *J. of Phys. and Chem. of Solids*, 64 (2003) 1365
[16] W.I. Łamajew, W.M. Gołowej, *Uzhgorod University Scientific Herald, Series Physics* 14 (2003) 27
[17] J.A. Hernandez, E.G. Camarillo, G. Munoz, C.J. Flores, E.B. Cabrera, F. Jaque, J.J. Romero, J. Garcia-Sole, H.S. Murrieta, *Opt. Mat*. 17(2001) 491
[18] G.B. Loutts, M. Warren, L. Taylor, R.R. Rakhimov, H.R. Ries, and G. Miller, *Phys. Rev. B*, 57 (7) (1998) 3706
[19] J.T. Randall, M.H.F. Wilkins, *Proc. Roy. Soc. London* A184 (1945), 366
[20] W. Drozdowski, K.R. Przegiętka, A.J. Wojtowicz, H.L. Oczkowski, *Acta Phys. Pol*. A95 (1999), 251
[21] A. Shengelaya, Guo-mang Zhoo, H. Koller, K.A. Muller, *Phys. Rev. Lett*., 77 (1996) 5296
[22] S.M. Kaczmarek, G. Boulon, *Opt. Mat*. 24 (2003) 151
[23] S.M. Kaczmarek, W. Chen, G. Boulon, M. Wabia*, The European Physical Journal Applied Physics*, in the print
[24] I. Ardelean, M. Peteanu, S. Filip, V. Simon and I. Todor, *Sol. State Comm*., vol. 105 (5) (1998) 339
[25] A. Abragam and B. Bleaney in: "*Electron Paramagnetic Resonance of Transition Ions*" (Clarendon, Oxford, 1970)
[26] M. Moreno, F. Rodriguez, J.A. Aramburu, F. Jaque, F.J. Lopez, Phys. Rev. B 28 (1983) 6100
[27] F.M. Ezz-Eldin, N.A. Elalaily, H.A. El-Batal and N.A. Ghoneim, *Radiat. Phys. Chem*., 48 (5) (1996) 659
[28] B. Beekenkamp, *Ph. D. thesis*, Technical University, Netherlands, 1966
[29] Gh. Ilonca, I. Ardelean and O. Cozar, *J. Phys*., 49 (1988) C8-1107
[30] I. Ardelean, Gh. Ilonca and O. Cozar, *Rev. Roum. Phys*., 33 (1988) 179
[31] V. Cerny, B. Petrova and M. Furmar, *J. Non-Cryst. Solids*, 161 (1995) 316
[32] U. Hummerich, H. Eilers, and W.M. Yen, Chem. Phys. Lett. 213 (1993) 163
[33] F.J. Lopez, M. Aguilar, and F. Agullo-Lopez, *Phys. Rev. B* 23 (6) (1981) 3041
[34] D. Ehrentraut, M. Pollnau, and S. Kuck, *Appl. Phys. B* 75(1) (2002) 59
[35] T.C. Brunold, F.N. Hazenkamp, and H.U. Gudel, J. Am. Chem. Soc. 117 (1995) 5598
[36] I.N. Ogorodnikov, V.A. Pustovarov, L.I. Isaenko, E.I. Zinin and A.V. Kruzhalov, *NIMA* 448 (2000) 467
[37] J.R. Cameron, N. Suntharalingam, and G.N. Kenney, Thermoluminescent Dosimetry, The University of Wisconsin Press, Madison, 1968
[38] N. Miura, *Phosphors for x-rays and ionizing radiation*, in Phosphor Handbook, S. Shionoya and W.M. Yen, eds., CRC Press, Boca Raton, 1998, pp. 521-537
[39] M.J. Aitken, Thermoluminescence dating, Academic Press, London, 1985
[40] N.A. El-Faramway, S.U. El-Kameesy, A.El-Agramy and G. Metwally, *Rad. Phys. & Chem.*, 58 (2000) 9
[41] Kang-Soo Park, J.K. Ahn, D.J. Kim, H. K. Kim, Y.H. Hwang, D.S. Kim, M.H. Park, Jin-Joo Yoon and Jae-Young Leem, *J. Cryst. Growth* 249 (2003) 483
[42] G.I. Malovichko, V.G. Grachov, A.O. Matkovskii, *Sov. Phys. Solid State,* 33 (1991) 1107